



# Dual-modality imaging of endothelial progenitor cells transplanted after ischaemic photothrombotic stroke

Jie Ding<sup>a,1</sup>, Yi Zhang<sup>a,1</sup>, Cong-Xiao Wang<sup>a</sup>, Pei-Cheng Li<sup>b</sup>, Zhen Zhao<sup>a</sup>, Chao Wang<sup>c</sup>, Gao-Jun Teng<sup>a,\*</sup>

<sup>a</sup> Jiangsu Key Laboratory of Molecular and Functional Imaging, Department of Radiology, Zhongda Hospital, Medical School, Southeast University, Nanjing, 210009, China

<sup>b</sup> Department of Interventional Radiology, First Affiliated Hospital of Soochow University, Suzhou, 215006, China

<sup>c</sup> Key Laboratory of Developmental Genes and Human Disease, Ministry of Education, Institute of Life Sciences, Southeast University, Nanjing, 210096, China

## ARTICLE INFO

### Keywords:

Stroke  
Endothelial progenitor cell (EPC)  
Dual-modality imaging  
Magnetic resonance imaging (MRI)  
Bioluminescence imaging (BLI)

## ABSTRACT

**Aims:** Stroke is a refractory cerebral blood circulation disorder. Endothelial progenitor cells (EPCs) participate in the repair and regeneration of vascular injury through the combination of cell replacement and bystander effects. Here, we evaluated the biological function of EPCs in treating a mouse model of cerebral ischaemic stroke, using dual-mode bioluminescence and magnetic resonance imaging to trace EPCs *in vivo*.

**Main methods:** We constructed a viral vector with a luciferase-enhanced green fluorescent protein (*Luc-eGFP*) reporter gene for bioluminescence imaging (BLI) detection, and simultaneously synthesized the magnetic resonance imaging (MRI) contrast agent, nano-sized superparamagnetic iron oxide (USPIO), to co-label human umbilical cord blood-derived EPCs (hEPCs). The labelled hEPCs were transplanted into mice with stroke, and the biological behaviours of the cells *in-vivo* were studied using BLI and MRI, and methods of molecular biology and histology.

**Key findings:** Comparing the two cell transplantation routes by BLI confirmed that many cells transplanted via the left ventricular route homed to ischaemic brain tissue. The dual-modality-imaging showed the prognosis of *in-vivo* tracking cells after transplantation in ischaemic tissues at different time points. Histological staining and neurological function scores confirmed that EPC transplantation can improve the symptoms of nerve deficit in the mouse stroke model. Histological staining revealed that cell transplantation can lead to recovery of neurological function after stroke, via various processes. These include reduced blood brain barrier permeability, recovery of white matter and of myelin, and the enhancement of neurogenesis.

**Significance:** Dual-modality imaging revealed EPCs as potential candidates for the treatment of ischaemic stroke.

## 1. Introduction

With the accelerated process of population aging, cerebral ischaemic stroke has become an urgent public health issue. Revascularization and drug neuroprotection are the major treatment options used for cerebral stroke. Revascularization can be observed in the early stages of cerebral stroke, using intravenous thrombolysis or other thrombectomy. This restores blood supply in stroke infarction; however, few people can receive treatment within an effective time period [1,2]. Various neuroprotective drugs have resulted in relatively sound treatment effects in animal studies [3]. Their clinical effects, however, are yet to be confirmed. On the other hand, rebuilding

damaged cerebral tissues through stem cell transplantation has become a new alternative to treat cerebral stroke [4,5].

Endothelial progenitor cells (EPCs), the precursor cells of endothelial cells, participate in embryonic vasculogenesis. Under many physiological and pathological states, EPCs function by mobilizing cells from marrow into peripheral blood circulation [6]. The features of EPCs, such as migration, homing and vasculogenesis. Indicate their potential for use in transplantation therapy for various diseases [7]. Preclinical studies related to EPCs, such as tracing prognosis of transplanted cells noninvasively *in vivo*, monitoring cell transmission in real time, examining whether transplanted cells can reach damaged areas, and subsequently understanding cell differentiation and proliferation

\* Corresponding author. Department of Radiology, Zhongda Hospital, Southeast University, #87 Dingjiaqiao Road, Nanjing, 210009, China. Tel.: +86 25 83272121; fax: +86 25 83311083.

E-mail addresses: [gjteng@vip.sina.com](mailto:gjteng@vip.sina.com), [gjteng@seu.edu.cn](mailto:gjteng@seu.edu.cn) (G.-J. Teng).

<sup>1</sup> Jie Ding and Yi Zhang contributed equally to this work.

<https://doi.org/10.1016/j.lfs.2019.116774>

Received 3 June 2019; Received in revised form 13 August 2019; Accepted 15 August 2019

Available online 02 November 2019

0024-3205/ © 2019 Published by Elsevier Inc.

[8], will all help to explain the processes whereby EPCs function, and the mechanisms involved in vasculogenesis. In a previous study [9], we separated, cultivated and identified EPCs from the umbilical blood of newborns, and packaged them to obtain virions carrying *Luc-eGFP* dual reporter genes. The EPCs were then marked via infectious virions for transplantation into mice with ischaemic stroke. Bioluminescence imaging was used for non-invasive and real-time monitoring of cell status. It was verified that EPCs can be used as a transplantation treatment for mice with ischaemic stroke, to improve behavioural defects, reduce infarction size, promote angiogenesis and neurogenesis in the infarction area, and reduce apoptosis. The primary results showed that EPCs are a promising and ideal transplantation cell source for ischaemic cerebral stroke [9].

However, bioluminescence imaging alone is insufficient. Some studies have focused on improving the technology used in cell labelling, or developing jointly applicable imaging modes based on different imaging principles [10,11]. Here, we have adopted the latter strategy, in which multiple imaging modes are combined to make optimal use of the strengths of each method, and to offset the shortcomings of single-mode imaging. This makes it possible to obtain the most comprehensive information about the targets of interest. In this study, our objective was to evaluate a dual-imaging approach: EPCs from umbilical blood were dual labelled, and BLI and MRI dual-mode imaging was developed and tested on a cellular level using a stroke animal model, to examine biological functions after EPC transplantation. We aimed to address two key questions: i) Is dual-modality imaging a viable approach for studying EPC homing? and ii) Do EPCs home in on the stroke area, and do they improve prognosis?

## 2. Materials and methods

### 2.1. Study design

Firstly, we compared two methods of EPC delivery, via the left ventricular vein and via the caudal vein. Based on this comparison, all later experiments applied the better delivery method. We then labelled EPCs for dual-modality imaging and checked the viability of the labelled cells *in vitro*. Next, labelled cells were transplanted into an ischaemic photothrombotic stroke mouse model. Dual-modality imaging was performed on this model to track cell homing, which was the focus of current work.

We then tested both the model mice treated with labelled EPCs and the control mice (stroke mice with no EPC treatment) using behavioural experiments. We also sacrificed some mice in both groups, sampled the brain tissues of the infarction area and surrounding tissues, and evaluated the neural functioning of these samples. In brief, we studied behaviour, permeability of the blood brain barrier (BBB), morphology and neurobiological markers to determine whether EPC treatment improved prognosis.

### 2.2. Cell preparation

Blood from a human umbilical cord was obtained from Zhongda Hospital affiliated to Southeast University, Nanjing, China. Signed informed consent and permission from the Ethics Committee were obtained. We performed hEPC culture isolation and identification as previously described [9].

### 2.3. Dual reporter chronic virion packaging and hEPC tagging

The procedure used for this experiment was performed as previously described [8]; however, the virion-infected hEPCs were referred to as V-hEPCs in the previous study.

### 2.4. SPION synthesis and characterization

The coprecipitation method was used to prepare superparamagnetic iron oxide nanoparticles (SPIONs). The mixed solution of  $\text{FeCl}_3 \cdot 6\text{H}_2\text{O}$  (20 mL, 1 mol/L) and  $\text{FeCl}_2 \cdot 4\text{H}_2\text{O}$  (20 mL, 0.5 mol/L) was added to HCl (0.2 mol/L), followed by stirring in a constant-temperature magnetic stirrer. A 10 mL volume of 26.5% ammonium hydroxide was added dropwise to the stirring solution and allowed to mix for 15 min. Ammonium hydroxide of the same concentration was slowly added dropwise to achieve a pH of 10, and a temperature of 60 °C was used for the 3 h continuous reaction. After cooling, the solution was centrifuged at  $7000 \times g$  for 20 min at 25 °C, to remove large particles. A dialysis membrane with a 50 000-molecular weight cut-off was used to remove the residues from the supernatant. Ultrasonic oscillation was conducted for 5 min and the bagged solution (after dialysis) was placed under a vacuum dryer at 60 °C (Jie Cheng Experimental Apparatus, Shanghai, China) for vacuum drying. The remnant was then packaged for sterilization and stored at 4 °C until use. For the SPIONs and polylysine (PLL) coupling, 1% PLL was added to the prepared SPIONs water solution, and stirred for 2 h. The magnetic separation method was adopted for washing, and the coupled PLL-SPIONs were dissolved in pure water with 3 mg/mL iron. The solution was stored at 4 °C prior to use. A transmission electron microscope was used to examine the morphological features of the coupled PLL-SPIONs.

### 2.5. V-hEPC tagging

V-hEPCs with relatively stable growth were used for SPION tagging. Based on the literature and pre-experiment results, the prepared PLL-SPIONs were added to EGM-2 culture medium, with a final iron concentration of 3 µg/mL. The solution was added to a culture box and incubated at 37 °C with 5%  $\text{CO}_2$ . Prussian blue staining was conducted 24 h after incubation, to confirm the efficiency of SPION tagging by v-hEPCs. Phosphate buffer solution (PBS) was used to wash the cells with 4% paraformaldehyde for 30 min prior to fixation, followed by two washes with DDW. Freshly prepared and equivalent volumes of 10% potassium ferrocyanide and 4% paraformaldehyde were added and staining allowed for 20 min. The cells were then observed under a microscope. As iron oxide is indicated by a blue colour; when this was obtained, a wash with distilled water was performed, followed by re-staining with nuclear fast red. The excitation light source was set to blue in the fluorescence microscope, to detect the expression of green fluorescence protein (GFP). hEPCs jointly tagged with chronic virions and SPIONs were referred to as D-hEPCs.

### 2.6. Mouse focal cerebral ischaemic stroke model prepared by photochemical method

BALB/c (nu/nu) mice were anaesthetised by intraperitoneal injection of pentobarbital sodium (0.03 mL/10 g). An electric hair clipper was used to remove hair from the head of mice. Intraperitoneal injection of rose-bengal stain (1 mg/10 g) was administered, and the abdomen gently rubbed to promote absorption. The mouse was fixed on the operation table in a prone position. The head skin was cut open after sterilization to clean the connective tissues at the skull surface to expose the bregma. The bregma was used as the base point, and the site of infarction was situated 2 mm below this, on the right side. A 3000 K cold light source was illuminated for 15 min to form illuminated local brain tissue infarction. After the operation, the head skin was seamed, and the mouse placed on a heating pad. Following revival, the mouse was returned to the cage. In the sham operation group, no injection of rose-bengal stain was administered; however, other procedures remained the same.

## 2.7. Cell administration

Scheme 1: V-hEPCs were transplanted into the stroked mice via the left ventricle and caudal vein to compare cell homing via these transplantation routes. The experiment was conducted in 2 groups: a left ventricle cell transplantation group, and a caudal vein cell transplantation group. In each group, 3–5 mice with stroke were transplanted by injection with  $1 \times 10^6$  V-hEPCs (100  $\mu$ L). Cell transplantation occurred 24 h after stroke modelling.

Scheme 2: D-hEPCs were transplanted into the stroked mice via left ventricle, to observe BLI and MRI dual-mode imaging, and the effect of cell transplantation treatment. The experiment was conducted in 2 groups: a D-hEPC transplantation treatment group via left ventricle, and a PBS injection control group via left ventricle. In each group, 3–5 mice with were transplanted by injection with  $1 \times 10^6$  D-hEPCs (100  $\mu$ L), and cell transplantation or PBS intervention was performed 24 h after stroke modelling.

Preparation of cell suspension for transplantation: under microscope observation, V-hEPCs or D-hEPCs in a sound state of growth were taken as the cell source for transplantation intervention. After cell trypsinization, centrifugation (800  $\times$ g, 5 min, 25  $^{\circ}$ C) was conducted followed by washing and then further centrifugation (800  $\times$ g, 5 min, 25  $^{\circ}$ C). After cell counting, PBS was used to regulate cell solubility and obtain a  $1 \times 10^7$ /mL cell suspension as standby.

## 2.8. BLI imaging

On days 1, 4 and 7 after V-hEPC transplantation, the small-animal *in vivo* bioluminescence imaging system (IVIS-Spectrum, PerkinElmer, Akron, OH, USA) was used to detect and tag the expression of reporter gene luciferase. This reflected the homing of cells transplanted via different routes. The mice were administered isoflurane (induction dosage 3% and maintenance dosage 1%) via inhalation as anaesthesia. Intraperitoneal injection of the bioluminescence imaging substrate, D-luciferin (150 mg/kg), was conducted. After 10 min, the prone position of mice was taken for placement on the IVIS-Spectrum indoor imaging platform. Data was then collected via *in vivo* imaging software. Based on the signal strength, a suitable exposure time was chosen to collect images. After imaging, the minimum and maximum values were regulated to generate an area equivalent to brain size as the region of interest (ROI). Quantitative analysis of the signal strength at the luminescence position (p/s/cm<sup>2</sup>/sr) was then conducted. Through double tagging of hEPCs, D-hEPCs were obtained. After D-hEPC transplantation, the *in vivo* imaging procedure followed the same operation used on days 1, 4, 7 and 14. The IVIS-Spectrum system was used to detect the homing in the brain tissues of the stroked mice administered EPCs via left ventricle. To conduct the *in vitro* imaging experiment,  $1 \times 10^6$ ,  $5 \times 10^5$ ,  $1 \times 10^5$  and  $5 \times 10^4$  D-hEPCs were inoculated in a 12-hole panel with different cell concentrations, and the  $1 \times 10^6$  untagged hEPCs was used as the negative control. The BLI substrate, D-luciferin (30 mg/mL, 150  $\mu$ L/hole), was added to the solution prior to a 5 min incubation period in the absence of light. The 12-hole panel was placed in the IVIS-Spectrum imaging system for cell level BLI.

## 2.9. MRI

MRI detection was conducted 24 h after SPION incubation of V-hEPCs. After normal cell trypsinization, 4% paraformaldehyde was added for fixation at 4  $^{\circ}$ C for 30 min. The cell counts were  $1 \times 10^6$ ,  $5 \times 10^5$ ,  $1 \times 10^5$  and  $5 \times 10^4$  per millilitre. Cells were then re-suspended in 0.5% agarose solution in a 60  $^{\circ}$ C water bath, to avoid agarose solidification. An Eppendorf tube containing the resuspended cells was quickly placed in the 4  $^{\circ}$ C refrigerator for cooling and removed once it had solidified. In a 7.0 T high-field-strength MR scanner, cells were tagged. The T2 STAR scanning sequence was adopted, with the following parameters: TR = 5000, 3000, 1500, 800, 400, and 200 ms;

TE = 11 ms; layer thickness = 1 mm; image collection time = 18 ms, FOV = 20 mm  $\times$  20 mm; and matrix = 256  $\times$  256. On days 1, 4, 7 and 14 following D-hEPC transplantation via left ventricle, MRI was conducted and isoflurane (induction dosage 3% and maintenance dosage 1%) was administered via inhalation as an anaesthesia. For the mouse MRI, a prone position was taken with the mouse head placed at the ring centre, and the anaesthesia dosage regulated to maintain the desired frequency of 25–35 times/min. The previously mentioned T2 STAR scanning parameters were used. On the 7th day following D-hEPC transplantation via left ventricle, MR T2 imaging was captured and compared to the control group to assess the changes of mouse infarction focus size. The T2 scanning parameters were as follows: RARE sequence; TR/TE: 1300 ms/7.5 ms; layer thickness = 1 mm; image collection time = 18; FOV 20 mm  $\times$  20 mm; and matrix = 256  $\times$  256. The FA value was measured in the ipsilesional corpus callosum with ParaVision 5.0 software (Bruker, Ettlingen, Germany).

## 2.10. Behavioural test

Neurological scoring (mNSS) was used to detect the movement, feeling, reflex movement and muscular tension of the different groups of mice with stroke, at different time points. On days 1, 4, 7 and 14, before and after stroke mouse modelling, the single blind method was used to score nervous function defects. At every time point, 3 mice were used, and a higher score represented a higher severity in damaged nerves. A foot-fault test was also used to detect neurological defects. In the experiment, the side of damage and the number of missed side steps were tested on the raised horizontal ladder. The number of foot faults experienced by mice in completing tasks at different time points after cell transplantation was calculated to evaluate the damage associated with feeling and movement functions.

## 2.11. BBB measurement

Evans blue solution at 2% (0.4 mL/100 g weight) was injected via the caudal vein, and the animals anaesthetised 1 h later. Normal saline was perfused often, via the left ventricle. The brain was isolated, and divided into left and right sections through the use of a blade to the midsagittal suture. The sections were weighed and submerged in 2 mL formamide solution, followed by 48 h of incubation in a constant temperature incubator. Following incubation, the sections were centrifuged for 8 min at 3000 rpm. The OD value of the supernatant was measured at a wave-length of 620 nm. The formamide solution was used as the blank control.

## 2.12. Tissue preparation and morphology immunohistochemistry

On the 14th day following cell transplantation, mice were sacrificed. Brain tissues were isolated after perfusion, rinsed then sliced after paraffin embedding. The embedded slices were deparaffinated with freshly prepared distilled water. Prussian blue (10% potassium ferrocyanide and 4% HCl for mixing) was used for 30 min of staining, after which 0.3% neutral red straining was added and allowed to sit for 5 min. PBS was then used for washing and a coverslip placed on the slide for observation under the microscope. Extra tissue slices were used for anti-MBP and anti-NeuN staining. After the slices were rinsed with PBS, they were submerged in 0.3% Triton X-100 PBS at room temperature. Anti-MBP monoclonal antibody (1:1000) and anti-NeuN monoclonal antibody (1:1000) were added to the cells and left for overnight incubation at 4  $^{\circ}$ C. For the anti-MBP staining group, biotin-tagged GaMigG was added and the ABC kit (Vector Laboratories, Inc., Burlingame, CA, USA) used for coloration. For the anti-NeuN staining group, FITC-tagged fluorescence GaMigG was added for DAPI staining, and observed using a fluorescence microscope.

2.13. Statistical analysis

All data are presented as mean ± standard deviation (SD). The data were tested for normality (IBM SPSS Statistics Version 19.0, Inc., Chicago, IL, USA), before being analysed using either parametric analysis of variance (ANOVA) or non-parametric tests. Data were analysed using either non-parametric Mann-Whitney U tests (two-tailed, 95% CI), or non-parametric Kruskal-Wallis tests (two-tailed, 95% CI) and post-hoc tests (Dunn's multiple comparisons test) in GraphPad Prism Version 6.0 (GraphPad Software, Inc., San Diego, CA, USA). A significance threshold of  $p < 0.05$  was considered statistically significant.

3. Results

3.1. BLI evaluation of the homing of mice with stroke, after being injected with V-hEPCs via different routes

After transplantation via the left ventricle, the average bioluminescence signals at different time points were  $3.8 \times 10^5$ ,  $5.7 \times 10^4$ , and  $3.9 \times 10^3$  (p/s/cm<sup>2</sup>/sr), on days 1, 4 and 7, respectively, with the strongest signal appearing on the first day. With the passage of time following transplantation, the optical signal declined significantly. For the group that was administered the transplantation via the caudal vein, the average bioluminescence signals at different time points were  $4.8 \times 10^4$ ,  $5.6 \times 10^3$ , and  $2.3 \times 10^3$  (p/s/cm<sup>2</sup>/sr), on days 1, 4 and 7, respectively, with the strongest signal appearing on the first day. As time passed, the optical signal declined significantly (Fig. 1A). Homing of V-hEPCs to ischaemic brain tissues was observed via both routes. The number of transplanted cells homing to the brain via the ventriculus sinister outweighed the number via the caudal vein. A statistical difference was observed for the bioluminescence imaging values on days

1, 4 and 7 after cell transplantation (Fig. 1B).

3.2. hEPC double labelling and dual-mode imaging

V-hEPCs and the prepared PLL-SPIONS were co-incubated for 24 h. The final concentration of iron was 30 µg/mL, and the cells under double labelling were marked as D-hEPCs. D-hEPCs underwent BLI (Fig. 2A) and MRI (Fig. 2B) detection with different cell concentrations. In the experiment, cell concentrations from  $1 \times 10^6$  to  $5 \times 10^4$  were chosen for dual-mode imaging. Fig. 2A shows the BLI imaging signal, with signal strength increasing with increasing number of labelled cells (the signal strength of  $1 \times 10^6$  D-hEPCs reached  $10^8$  p/s/cm<sup>2</sup>/sr). Fig. 2B shows the MRI imaging signal, with signal strength indicating low luminance with increasing number of labelled cells. This demonstrated the special imaging features of the MRI T2 STAR sequence. D-hEPCs that were growing at a stable rate were chosen for detection by fluorescence and Prussian blue staining.

Fluorescence microscopic examination showed the GFP expression in D-hEPC cytoplasm (Fig. 2D). When compared to white light (Fig. 2C), GFP expression was evident in almost all double-labelled cells, re-confirming that virions could effectively label hEPCs. The cytoplasm stained with nuclear fast red displayed the colour red in the unlabelled hEPCs; however, almost all cytoplasm of D-hEPCs displayed the blue staining (Fig. 2E and F). Prussian blue staining therefore displayed a positive reaction, confirming the ability of hEPCs to take in iron, with almost 100% of the cells being labelled by SPIONS. The dual-mode imaging of D-hEPCs provided convincing evidence of its applicability for future *in-vivo* imaging of cell transplantation.

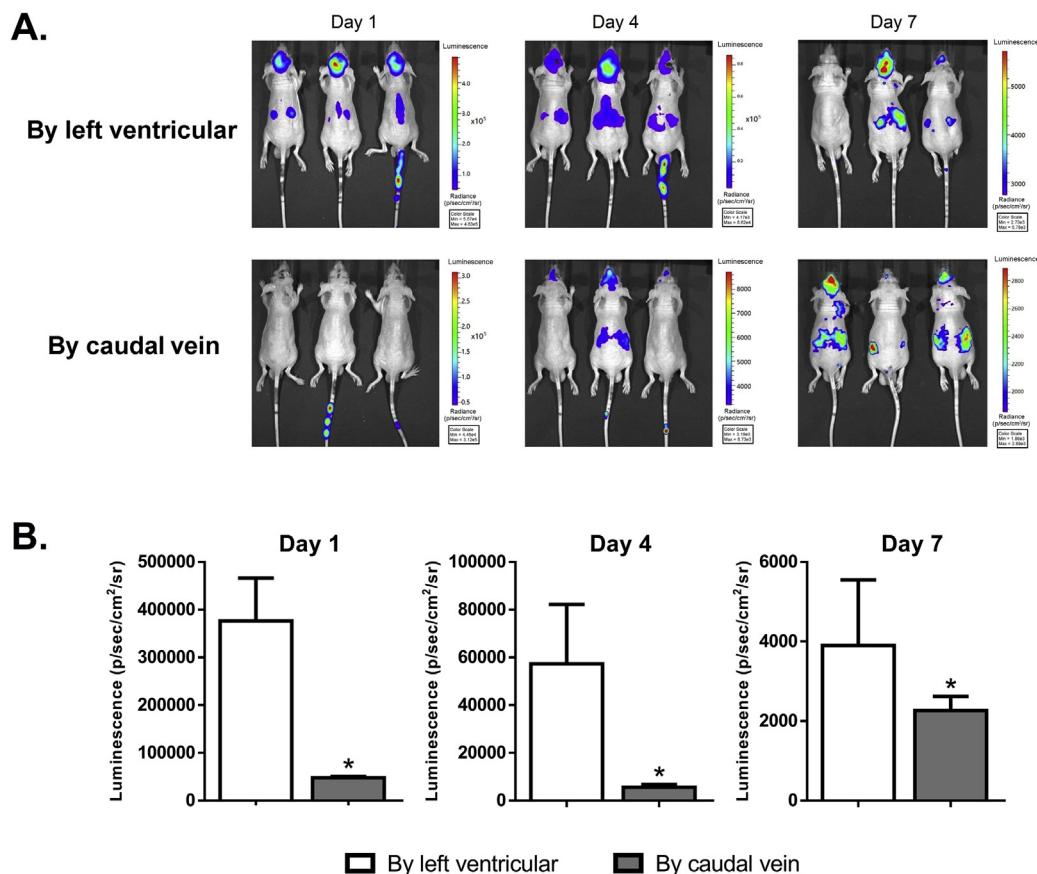
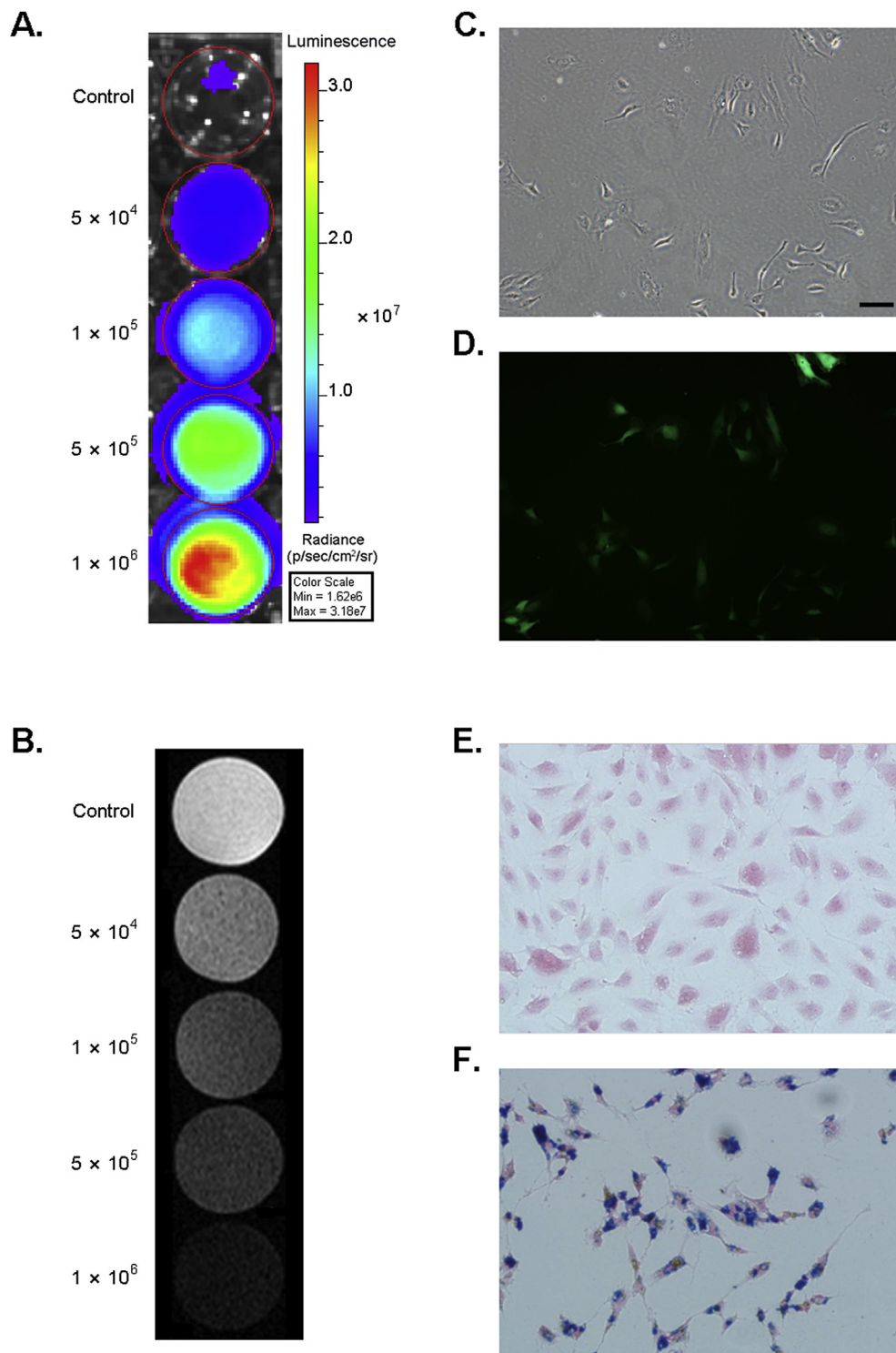


Fig. 1. (A) At days 1, 4 and 7 after cell transplantation, there were optical signals in the ischaemic brain tissues. (B) At days 1, 4 and 7, statistical analysis showed that the intensity of optical signals in the ischaemic brain tissues varied with the means of transplantation ( $p < 0.05$ ;  $n = 3$ ).



**Fig. 2.** (A) D-hEPC bioluminescence imaging (BLI) detection with different cell concentrations. (B) D-hEPC MRI detection with different cell concentrations. (C) Labelled D-hEPCs under light microscope. (D) Labelled D-hEPCs fluorescence detection (GFP). (E) Unlabelled hEPCs with Prussian blue staining. (F) Labelled D-hEPCs with Prussian blue staining. Scale bar: 50  $\mu\text{m}$ . (For interpretation of the references to colour in this figure legend, the reader is referred to the Web version of this article.)

### 3.3. Dual-mode tracing in stroked mice after D-hEPC transplantation through the left ventricle

After the mouse stroke model was established using the photochemical method, and 24 h had passed,  $1 \times 10^6$  D-hEPCs were transplanted via the left ventricle. On days 1, 4, 7 and 14, BLI and MRI were conducted. The BLI signal is shown in Fig. 3A. The day following D-

hEPC transplantation, the optical signals in the ischaemic brain tissues could be observed. With the passage of time, the bioluminescence signal became significantly reduced, and was consistent with the results of the injection with V-hEPCs. The MRI signal is shown in Fig. 3B. MR T2 STAR imaging revealed particularly low signals at the area with ischaemic tissues. On the first day following cell transplantation, the signal was the strongest. With the passage of time, the signal weakened;

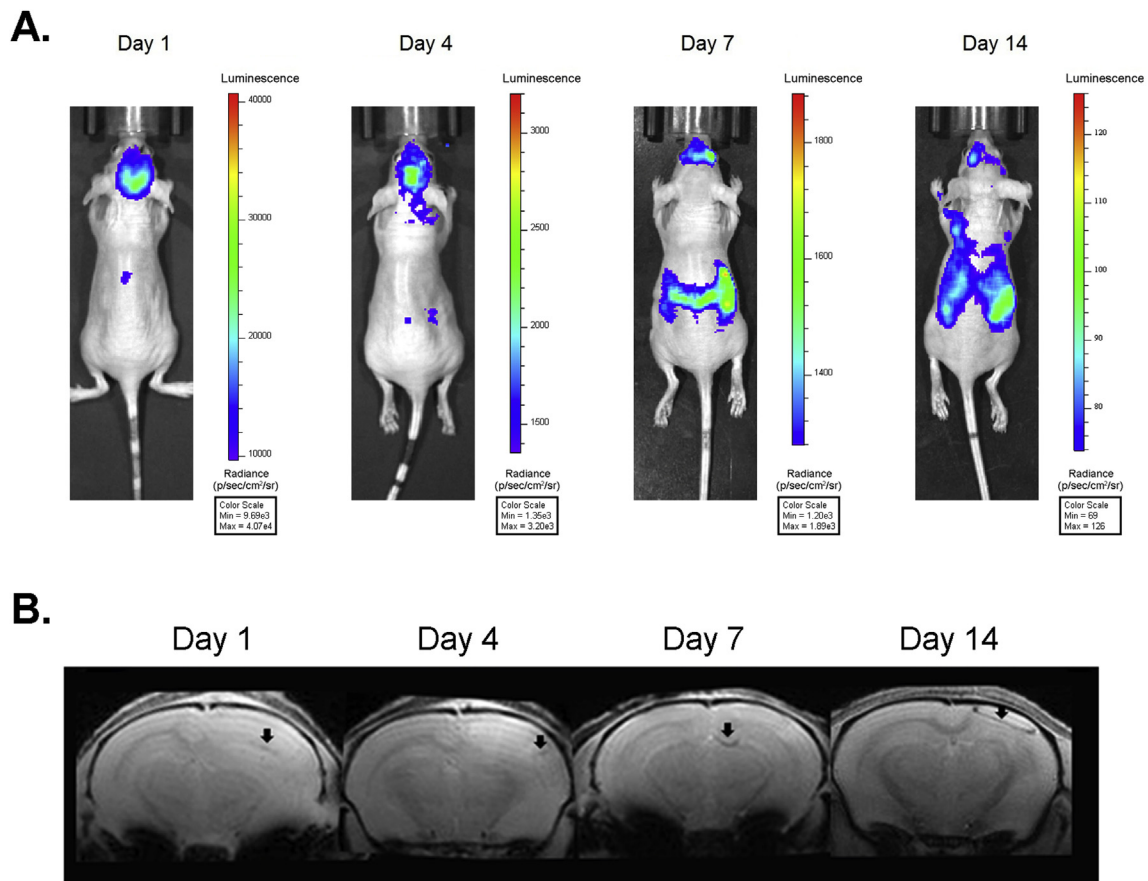


**Fig. 3.** (A) Bioluminescence imaging at different time points after D-hEPCs transplantation. (B) Magnetic resonance T2 STAR imaging at different time points after D-hEPC transplantation, as indicated by black arrows.

however, on day 14, the MR signal could still be observed.

### 3.4. Histopathological detection of D-hEPC homing to ischaemic brain tissues

On day 14 following cell transplantation, pathological detection was used to determine the homing status of D-hEPCs. Prussian blue staining revealed a blue-stained positive signal at the edge of the infarction (Fig. 4B and C). Meanwhile, immunofluorescence staining revealed GFP-positive signals around the infarction (Fig. 4D–F). Histological staining results verified that D-hEPCs could home to the periphery of ischaemic brain tissues.

### 3.5. D-hEPC transplantation reduces the volume of brain infarction focus in mice with stroke, and ultimately promotes their neural functional recovery

Through MR T2 imaging, the volume of brain infarction focus in mice 7 days after D-hEPC intervention was compared. As shown in Fig. 5A, when compared to the PBS control group, D-hEPC transplantation reduced the volume of the brain infarction focus ( $p < 0.05$ ). Tests were conducted (mNSS and intermittent claudication tests) on mice in the PBS control group and D-hEPC intervention group 1 d before modelling, and 1, 4, 7 and 14 d after modelling. This was to detect neurological function impairment (Fig. 5B and C). Results showed that D-hEPC transplantation could reduce the phenotype of behavioural defects among mice with stroke ( $p < 0.05$ ).

Through caudal vein administration of Evans blue, changes in blood brain barrier permeability after brain infarction in mice were compared, 4 d after D-hEPC intervention. As shown in Fig. 6A, D-hEPC transplantation reduced blood brain barrier permeability after brain

infarction, compared to the PBS control group ( $p < 0.05$ ). Through measurement of the FA value and the brain white-matter fibre tracts after rebuilding, MR diffusion tensor imaging (DTI) showed brain white-matter restoration in mice with stroke, 14 days after D-hEPC transplantation (Fig. 6B). On day 14 after cell transplantation, mice were sacrificed, followed by paraffin embedding, and slicing of brain tissues after perfusion. Histological staining detection of anti-MBP monoclonal antibody was conducted to observe myelin sheath restoration around the ischaemic focus. Results showed that the D-hEPC intervention group had enhanced myelin-sheath neogenesis around the ischaemic focus of mice with stroke ( $p < 0.05$ ) (Fig. 6C). Immunofluorescence NeuN staining also revealed that neurogenesis was promoted after D-hEPC intervention; the difference was significant compared to the control group ( $p < 0.05$ ) (Fig. 6D).

## 4. Discussion

Radionuclide imaging, optical imaging, and MR imaging are the three most common imaging modalities available for EPC tracing. Radioactive rays are of limited value for tracking proliferation and differentiation in cells, because of their short half-life [12]. MRI has several advantages that make it a good prospect for broad application in live-cell tracking: it lacks the limitations associated with ionizing radiation, has great depth and angle of detection, high spatial and temporal resolution, and allows easy clinical transformation. Presently, most of the contrast agents for stem cell MRI tracing are T2-contrast agents, based on iron oxide nanoparticles, including SPIONs, very small paramagnetic iron oxide (VSPIO), and ultra-small superparamagnetic iron oxide (USPIO), to name a few [13,14]. MRI technology can provide detailed anatomical localization in live cell tracing; however, its

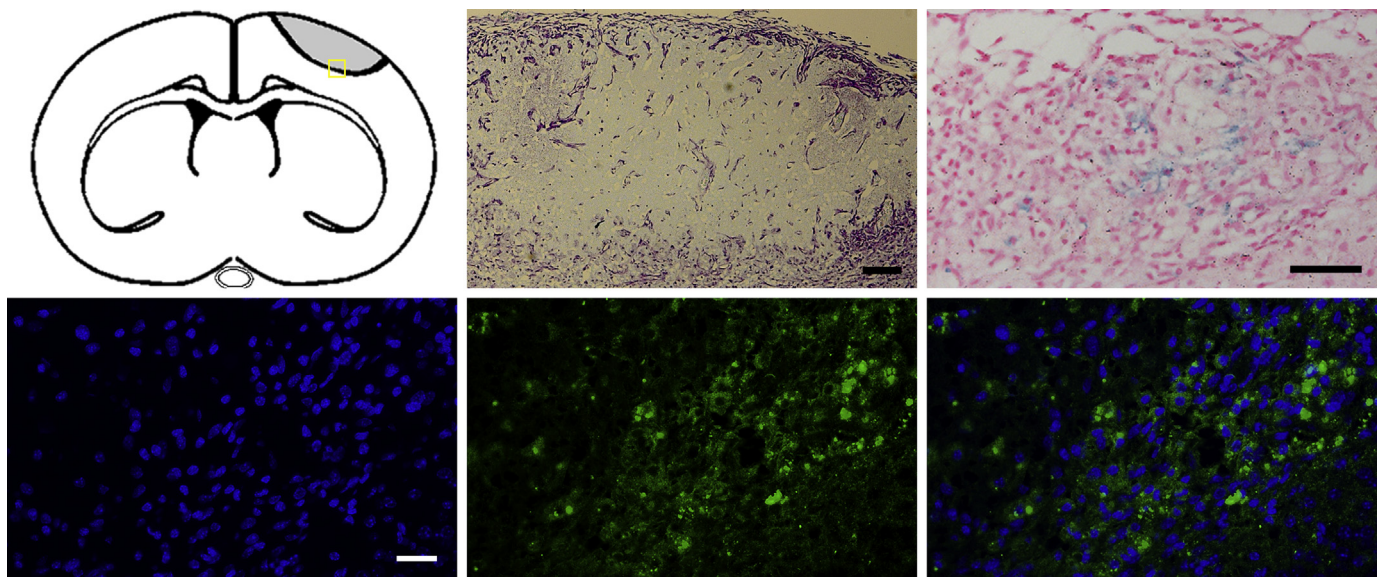


**Fig. 4.** (A) Chart of stroke mode in mice, with the grey area representing the infarction. Yellow square: sampling area. (B) Prussian blue staining. Scale bar: 100 µm. (C) Prussian blue staining. Scale bar: 50 µm. (D) Immunofluorescence, DAPI. Scale bar: 50 µm. (E) Immunofluorescence, anti-GFP. (F) Merge of (D) and (E). (For interpretation of the references to colour in this figure legend, the reader is referred to the Web version of this article.)

inherent low sensitivity has limited its further development. In addition, intracellular magnetic groups gradually decrease with the division and proliferation of stem cells, causing a dilution effect [15,16].

Optical imaging, including fluorescence imaging and BL imaging, has the advantages of not using radiation and of rapid, real-time and continuous monitoring. Thus, optical imaging shows good application prospects for use in stem-cell transplantation-tracing research and tumour drug-therapy evaluation. Through molecular biological manipulation, two reporter gene molecules, from fluorescent protein and luciferase, are fused and expressed. Infectious viral particles are obtained through the virus packaging system; these can be used in target-cell labelling and monitoring of imaging. Optical imaging has the advantages of being highly sensitive, highly specific, with low background detection; it therefore has broad application prospects in stem-cell marker imaging [10,17]. However, it is associated with poor light-wave

penetration, which results in low spatial resolution [18]. Therefore, optical imaging is better than MRI for cell tracing. MRI, however, has the advantage of high resolution, which is lacking in optical imaging. Therefore, combining MRI and BLI imaging modalities, which are non-invasive, promises to improve the sensitivity and spatial resolution of stem-cell tracing, and to allow improved evaluation of the biological behaviours of EPCs, such as localization, proliferation, differentiation, migration and outcome, and better monitoring after transplantation therapy.

In this experiment, umbilical cord blood-derived EPCs were isolated and cultured. Lentiviral particles carrying the reporter gene *Luc-eGFP* and high efficiency SPIONs were utilized. Non-invasive double-labelled hEPCs were monitored at the cell-level via BL and MR imaging. Transplanted cells were monitored in the mouse stroke model. We first used BLI to compare the homing of exogenous cells via different routes

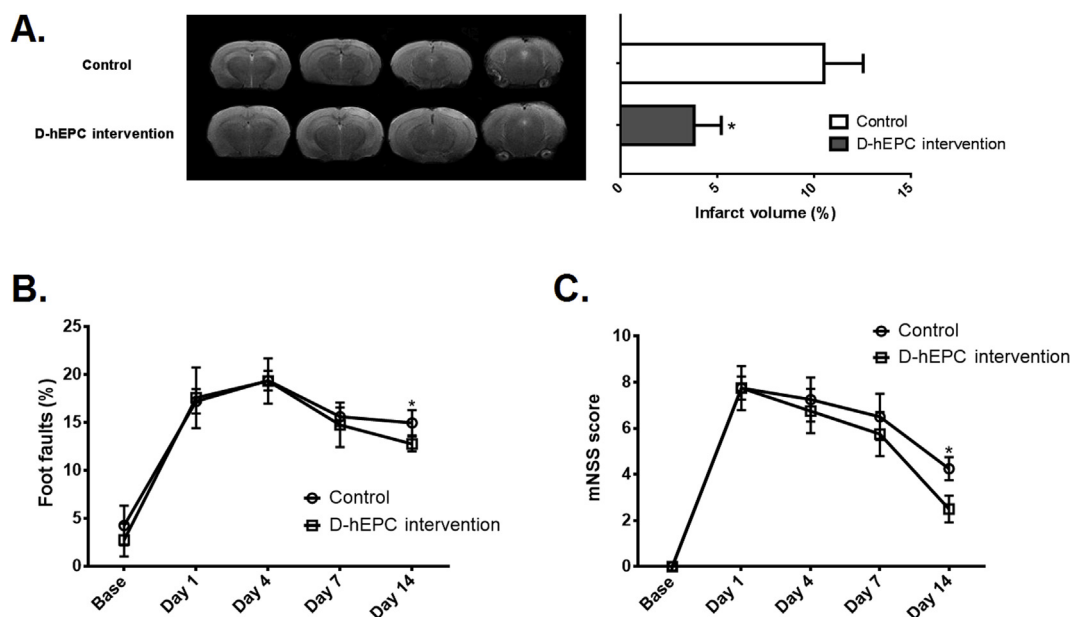


**Fig. 5.** D-hEPCs transplantation reduces the volume of (A) the brain infarction focus, (B) the foot-fault percentage, and (C) mNSS scores, in mice with stroke. D-hEPCs ultimately promote neural functional recovery in these mice ( $p < 0.05$ ;  $n = 3$ ).

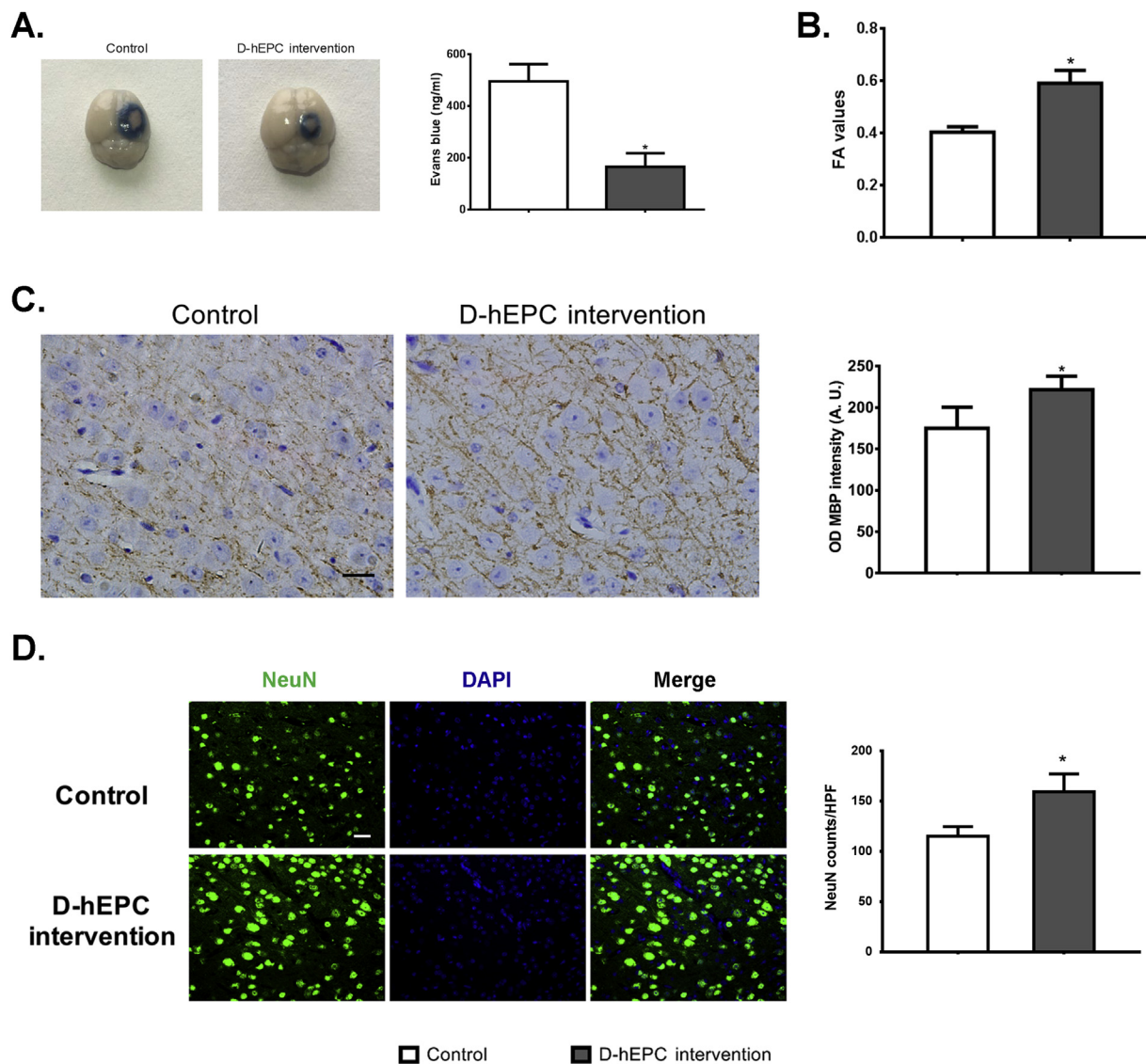


**Fig. 6.** D-hEPCs transplantation (A) improves the blood brain barrier, (B) promotes white-matter development, (C) promotes myelin-sheath neogenesis (C, Scale bar: 50  $\mu$ m), and (D) promotes neurogenesis (D, Scale bar: 50  $\mu$ m) ( $p < 0.05$ ;  $n = 3$ ).

in mice with stroke (Fig. 1). For the cells infused through the left ventricle, the number homing to ischaemic tissue was superior to that of the cells infused through the caudal vein. *In-vivo* imaging tracing allows the monitoring of exogenous cells that are transplanted, and can also answer the following questions: what is the final outcome of therapeutic stem cells? Can changing the local microenvironment of the brain through bioengineering methods attract more stem cells to home to brain tissues? What is the relationship between the types of protective factors released by stem cells, the functions of protective factors, and stem cell location? What are the differences in treatment effect of stem cells from different sources, and how can we select the optimal donor cells for stroke treatment? MRI and BLI make it possible to clarify these issues more comprehensively. Thus, it is possible to use transformed cells for cell therapy to treat stroke. This is a direction for our follow-up research.

The level of EPCs in the peripheral blood of healthy bodies is extremely low, and they are mainly found in the angiogenic region of marrow tissues. In some pathological states, EPCs may be released into the peripheral circulation by bone marrow, targeting the damaged vascular endothelium in ischaemic and hypoxic tissues [6]. After stroke, different types of brain-intrinsic cells interact to maintain, remodel, and repair brain-tissue functions. The neurovascular unit is a complex

network of interactions and interconnections among these cells, and includes neurons, astrocytes, microglia, endothelial cells, and extracellular spaces [19]. Brain endothelial cells are an important component of the vascular system, and are mainly responsible for selectively transporting molecules and cells, and releasing soluble nutrients for the surrounding brain parenchyma [20,21]. Therefore, the interaction between EPCs and brain-intrinsic cells plays an important role in neurovascular units. In this experiment, it was verified by histological staining and neurological function scores that transplanted EPCs play a positive role in recovery from stroke in mice. Our results indicate that EPCs can improve the symptoms of neurological deficits in mice with stroke (Fig. 5). We believe that the recovery of neurological function following cell transplantation after stroke is associated with the reduced permeability of the BBB, the recovery of white matter and myelin, and the enhancement of neuroneogenesis (Fig. 6). We assumed that through the combination of the cell replacement effect and bystander effect, EPCs can engage in vascular injury repair and regeneration. This suggests they can be used as a potential candidate for the treatment of ischaemic stroke.

However, the current study lacked an in-depth analysis of the mechanisms involved. We did not study the paracrine effect of EPCs, focus on discovering potential mediators, or analyse the EPC signalling

mechanism. Although we were unable to evaluate these mechanisms within this study, our follow-up research aims to achieve this. Based on the existing experimental results, the follow-up research will aim to improve the tolerance of cells to hypoxia, by modifying the EPC gene, improve the local microenvironment of ischaemic brain tissue to increase the number of homing cells transplanted, and improve the viability of EPCs in infarcted brain tissue [22].

## 5. Conclusions

Based on our findings, we propose that EPCs are the ideal source of transplantation cells for patients with stroke, because the blood brain barrier of mice improved with EPCs after stroke, and nervous system remyelination was promoted, thereby regulating neurovascular unit functions. In the present study, human EPCs were used as transplant donor cells, and BALB/c (nu/nu) mice as the cell transplantation host. There is the potential for immune rejection after EPC transplantation. This research did not explore the role of inflammatory mediators and inflammatory responses in treatment. Therefore, another important research direction is to evaluate potential inflammatory factors related to EPC transplantation and clarify the EPC transplantation-related signalling pathways.

## Funding

This research was supported by the Fundamental Research Funds for the Central Universities [grant number 2242019k30035] from the National Natural Science Foundation of China, the National Key Research and Development Program of China [grant number 2017YFA0104302] and the Natural Science Foundation of Jiangsu Province of China [grant number BK20160703].

## Data statement

The datasets used and/or analysed during the current study are available from the corresponding author on reasonable request.

## Author contribution

J. Ding, Y. Zhang, C.-X. Wang, P.-C. Li and Z. Zhao performed the experiments. J. Ding and C. Wang analysed data and wrote the manuscript. C. Wang edited the figures. G.-J. Teng designed the research, provided key advice and essential assistance, finished the paper and provided funds for the project. All authors have discussed the results and approved the manuscript.

## Declaration of competing interest

There is no competing interest to declare.

## Acknowledgements

We thank EdiTar Bio-tech Ltd. (Nanking, China) for language rephrasing and polishing.

## References

- [1] K.R. Lees, et al., Time to treatment with intravenous alteplase and outcome in stroke: an updated pooled analysis of ECASS, ATLANTIS, NINDS, and EPITHET trials, *Lancet* 375 (9727) (2010) 1695–1703.
- [2] V.L. Roger, et al., Executive summary: heart disease and stroke statistics–2012 update: a report from the American Heart Association, *Circulation* 125 (1) (2012) 188–197.
- [3] A. Moretti, et al., Neuroprotection for ischaemic stroke: current status and challenges, *Pharmacol. Ther.* 146 (2015) 23–34.
- [4] A.C. Boese, et al., Neural stem cell therapy for subacute and chronic ischemic stroke, *Stem Cell Res. Ther.* 9 (1) (2018) 154.
- [5] A. Eckert, et al., Bystander effect fuels human induced pluripotent stem cell-derived neural stem cells to quickly attenuate early stage neurological deficits after stroke, *Stem Cell. Transl. Med.* 4 (7) (2015) 841–851.
- [6] T. Asahara, et al., Isolation of putative progenitor endothelial cells for angiogenesis, *Science* 275 (5302) (1997) 964–967.
- [7] G. Esquivia, A. Grayston, A. Rosell, et al., Revascularization and endothelial progenitor cells in stroke, *Am. J. Physiol. Cell Physiol.* 315 (5) (2018 Nov 1) C664–C674, <https://doi.org/10.1152/ajpcell.00200.2018> Epub 2018 Aug 22.
- [8] J. Ding, et al., Dual-reporter imaging and its potential application in tracking studies, *J. Fluoresc.* 26 (1) (2016) 75–80.
- [9] J. Ding, et al., Bioluminescence imaging of transplanted human endothelial colony-forming cells in an ischemic mouse model, *Brain Res.* 1642 (2016) 209–218.
- [10] N. Sun, et al., Long term non-invasive imaging of embryonic stem cells using reporter genes, *Nat. Protoc.* 4 (8) (2009) 1192–1201.
- [11] T.R. Doeppner, D.M. Hermann, Stem cell-based treatments against stroke: observations from human proof-of-concept studies and considerations regarding clinical applicability, *Front. Cell. Neurosci.* 8 (2014) 357.
- [12] M. Hofmann, et al., Monitoring of bone marrow cell homing into the infarcted human myocardium, *Circulation* 111 (17) (2005) 2198–2202.
- [13] S. Ju, et al., In vivo MR tracking of mesenchymal stem cells in rat liver after intrasplenic transplantation, *Radiology* 245 (1) (2007) 206–215.
- [14] S. Ju, et al., In vitro labeling and MRI of mesenchymal stem cells from human umbilical cord blood, *Magn. Reson. Imaging* 24 (5) (2006) 611–617.
- [15] J.W. Bulte, D.L. Kraitchman, Iron oxide MR contrast agents for molecular and cellular imaging, *NMR Biomed.* 17 (7) (2004) 484–499.
- [16] E.T. Ahrens, et al., In vivo imaging platform for tracking immunotherapeutic cells, *Nat. Biotechnol.* 23 (8) (2005) 983–987.
- [17] H.K. Yip, et al., Level and value of circulating endothelial progenitor cells in patients after acute ischemic stroke, *Stroke* 39 (1) (2008) 69–74.
- [18] N. Shah, et al., Noninvasive functional optical spectroscopy of human breast tissue, *Proc. Natl. Acad. Sci. U. S. A.* 98 (8) (2001) 4420–4425.
- [19] E.H. Lo, G.A. Rosenberg, The neurovascular unit in health and disease: introduction, *Stroke* 40 (3 Suppl) (2009) S2–S3.
- [20] N. Weiss, et al., The blood-brain barrier in brain homeostasis and neurological diseases, *Biochim. Biophys. Acta* 1788 (4) (2009) 842–857.
- [21] S. Guo, et al., Neuroprotection via matrix-trophic coupling between cerebral endothelial cells and neurons, *Proc. Natl. Acad. Sci. U. S. A.* 105 (21) (2008) 7582–7587.
- [22] F. Ma, et al., Endothelial progenitor cells and revascularization following stroke, *Brain Res.* 1623 (2015) 150–159.